Dynamics of an ultracold cascade three-level atom interacting with a two-mode cavity field

2002 J. Opt. B: Quantum Semiclass. Opt. 4 30

(http://iopscience.iop.org/1464-4266/4/1/305)

INSTITUTE OF PHYSICS PUBLISHING JOURNAL OF OPTICS B: QUANTUM AND SEMICLASSICAL OPTICS
J. Opt. B: Quantum Semiclass. Opt. **4** (2002) 30–36 PII: S1464-4266(02)24930-7

Dynamics of an ultracold cascade three-level atom interacting with a two-mode cavity field

Zhi-Ming Zhang[1,2,4], **Sien Chi**[1] **and Bing-Chung Cheng**[3]

[1] Institute of Electro-Optical Engineering, National Chiao Tung University, Hsinchu 30050, Taiwan, China
[2] Department of Physics, Shanghai Jiao Tong University, Shanghai 200030, China
[3] Department of Physics, Fu-Jen Catholic University, Taipei, Taiwan, China

E-mail: zmzhang56@hotmail.com

Received 17 May 2001, in final form 4 December 2001
Published 14 January 2002
Online at stacks.iop.org/JOptB/4/30

Abstract
The interaction between an ultracold cascade three-level atom and a two-mode cavity field has been studied. The effects of the centre-of-mass motion, the cavity length, the coupling constants, the initial field states and the initial field intensity on the atomic dynamics have been examined. We have found that the population probabilities show dependence on the interaction time in the fast-atom region while they show dependence on the interaction length in the slow-atom region. The variations of the probabilities versus the cavity length show resonant peaks, and the peaks become sharper as the atom moves more slowly. The coupling constants, the initial field states and the initial field intensity also influence the atomic dynamics significantly. The two transitions are competitive for the atomic probability in the middle state, while they are cooperative for that in the lower state.

Keywords: Atom–field interaction, ultracold atom, atomic dynamics

1. Introduction

With the development of laser cooling and trapping techniques [1], ultracold atoms have been obtained. Many new concepts and new phenomena, that involve ultracold atoms, are proposed or observed. Among them are atom optics [2], Bose–Einstein condensation [3], atom lasers [4], nonlinear atom optics [5], nonlinear optics of matter waves [6] and maser action [7–9]. In these phenomena, the interaction between ultracold atoms and quantum radiation fields plays an important role [10], and the quantization of the centre-of-mass (c.m.) motion of atoms must be taken into account in studies on this kind of interaction. In this paper we study the interaction between an ultracold cascade three-level atom and a two-mode cavity field. The aim is to examine the effects of the c.m. motion quantization, the cavity length, the coupling constants between the atom and the field, the initial field states and the initial field intensity on the atomic dynamics. The organization of this paper is as follows. In order to compare the results of this paper with previous studies we briefly review some results on the interaction of a cascade three-level atom with a two-mode cavity field, but without considering the atomic c.m. motion quantization (section 2). In section 3 we study the same interaction model, but we consider a situation in which the atom moves very slowly and its c.m. motion is described quantum mechanically. We treat the atom–field interaction as a scattering process, and find the reflection amplitudes and the transmission amplitudes, which are used for the calculations of related physical quantities. In sections 4 and 5 we study the atomic dynamics analytically and numerically, respectively. We examine the influences of the parameters mentioned above on the atomic dynamics. Section 6 is a brief summary of our main results.

[4] Author to whom correspondence should be addressed.

2. Model without c.m. motion quantization

We consider a micromaser-like experiment [14]. A well defined two-mode field is prepared in a high-quality-factor cavity. A three-level atom, initially prepared in a suitable state, is injected into the cavity and interacts with the cavity field. After the interaction, the atom exits the cavity and its population probabilities among its internal states can be measured with a state-selective field ionization technique.

In order to compare the results of this paper with previous studies, we first briefly review some results on the interaction of a cascade three-level atom with a two-mode cavity field (figure 1), without considering the c.m. motion quantization. Under the dipole approximation and the rotating wave approximation, and in the interaction picture, the Hamiltonian for the whole system (atom + field) reads (take $\hbar = 1$)

$$V = g_1(a_1^+|b\rangle\langle a| + |a\rangle\langle b|a_1) + g_2(a_2^+|c\rangle\langle b| + |b\rangle\langle c|a_2), \quad (1)$$

where $|a\rangle$, $|b\rangle$ and $|c\rangle$ are the three states of the atom with their energies satisfying $\omega_a > \omega_b > \omega_c$. a_i $(i = 1, 2)$ and a_i^+ are the annihilation and creation operators of mode i of the cavity field. g_1 (g_2) is the coupling constant between mode 1 (2) of the cavity field and the atomic transition $|a\rangle \leftrightarrow |b\rangle$ $(|b\rangle \leftrightarrow |c\rangle)$. Here we have assumed that mode 1 (2) of the cavity field is resonant with the atomic transition $|a\rangle \leftrightarrow |b\rangle$ $(|b\rangle \leftrightarrow |c\rangle)$. The dynamics of the system can be described by the state vector

$$|\Psi_{n_1,n_2}(t)\rangle = C_{a,n_1,n_2}(t)|a, n_1, n_2\rangle + C_{b,n_1+1,n_2}(t)|b, n_1+1, n_2\rangle + C_{c,n_1+1,n_2+1}(t)|c, n_1+1, n_2+1\rangle, \quad (2)$$

where n_1 and n_2 are the numbers of photons in modes 1 and 2, respectively. $C_{x,n_1,n_2}(x = a, b, c)$ is the probability amplitude of the system being in the state $|x, n_1, n_2\rangle$. Substituting (1) and (2) into the Schrödinger equation we obtain

$$\dot{C}_{a,n_1,n_2}(t) = -\mathrm{i}d_1(n_1)C_{b,n_1+1,n_2}(t), \quad (3)$$

$$\dot{C}_{b,n_1+1,n_2}(t) = -\mathrm{i}[d_1(n_1)C_{a,n_1,n_2}(t) + d_2(n_2)C_{c,n_1+1,n_2+1}(t)], \quad (4)$$

$$\dot{C}_{c,n_1+1,n_2+1}(t) = -\mathrm{i}d_2(n_2)C_{b,n_1+1,n_2}(t), \quad (5)$$

where $d_i(n_i) = g_i\sqrt{n_i+1}$ $(i = 1, 2)$. Assuming the initial condition

$$C_{a,n_1,n_2}(0) = 1, \qquad C_{b,n_1+1,n_2}(0) = C_{c,n_1+1,n_2+1}(t) = 0, \quad (6)$$

we find the solution

$$C_{a,n_1,n_2}(t) = \left(\frac{d_1(n_1)}{\Omega_{n_1,n_2}}\right)^2\left[\left(\frac{d_2(n_2)}{d_1(n_1)}\right)^2 + \cos(\Omega_{n_1,n_2}t)\right], \quad (7)$$

$$C_{b,n_1+1,n_2}(t) = -\mathrm{i}\frac{d_1(n_1)}{\Omega_{n_1,n_2}}\sin(\Omega_{n_1,n_2}t), \quad (8)$$

$$C_{c,n_1+1,n_2+1}(t) = -\frac{d_1(n_1)d_2(n_2)}{\Omega_{n_1,n_2}^2}[1 - \cos(\Omega_{n_1,n_2}t)], \quad (9)$$

where $\Omega_{n_1,n_2} = \sqrt{d_1^2(n_1) + d_2^2(n_2)}$. When $g_2 = 0$, equations (7)–(9) can be reduced to $C_{a,n_1,n_2}(t) = \cos\left(g_1\sqrt{n_1+1}t\right)$, $C_{b,n_1+1,n_2}(t) = -\mathrm{i}\sin\left(g_1\sqrt{n_1+1}t\right)$ and $C_{c,n_1+1,n_2+1}(t) = 0$. This is just the result for the standard Jaynes–Cummings model [11], and many theoretical predictions in the Jaynes–Cummings model, for example the Rabi oscillation and the collapse-revival of atomic dynamics, the sub-Poissonian photon statistics of the cavity field and so on, have been confirmed in experiments [11, 14, 15].

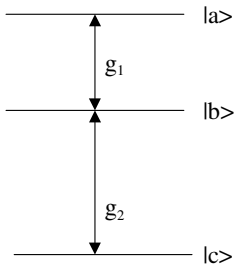

Figure 1. Scheme of the interaction between a cascade three-level atom and a two-mode cavity field.

3. Model with c.m. motion quantization

It is well known from quantum mechanics that the wavelength of the de Broglie wave of an atom (or any other matter) increases when the atomic momentum decreases, and the c.m. motion of the atom must be described quantum mechanically when the atom is slow enough. With the development of laser cooling and trapping techniques [1], ultracold (or ultraslow) atoms have been obtained. It becomes reasonable to ask what happens when the atoms are so cold that their c.m. motion has to be described quantum mechanically. How is the interaction between the atoms and radiation fields affected when the atomic kinetic energy is smaller than the atom–field interaction energy? Horache *et al* and Englert *et al* [10] studied the interaction between slow atoms and cavity fields, and showed that the atoms may be reflected by the cavity field when the atoms are slow enough. Scully *et al* [7] studied the micromaser injected with ultracold atoms and predicted a new kind of induced emission: the maser action. Loffler *et al* [7] made some considerations for observing the maser action in experiments. In these papers it is assumed that the atom–field interaction takes the form of the standard Jaynes–Cummings model [11], i.e. an interaction between a two-level atom and a single-mode cavity field. In this paper we study the interaction between an ultracold cascade three-level atom and a two-mode cavity field, and examine the effects of the atomic c.m. motion quantization and other factors on the atomic dynamics.

Here we still consider the micromaser-like experiment as described at the beginning of the previous section, but we now consider the situation in which the atom moves very slowly, and we describe the atomic c.m. motion quantum mechanically. Assume that the atom moves along the z-direction, then the Hamiltonian for the whole system (atom + field) reads

$$H = \frac{p_z^2}{2M} + u(z)V, \quad (10)$$

where V is given by equation (1), M is the atomic mass, p_z is the atomic c.m. momentum operator and $u(z)$ is the cavity mode function. In the following we shall first find the eigenvalues and eigenvectors (the dressed states) of V and then expand the states of the whole system with these dressed states.

The eigenequation of V can be written as

$$V|D^{(i)}_{n_1,n_2}\rangle = V^{(i)}_{n_1,n_2}|D^{(i)}_{n_1,n_2}\rangle, \tag{11}$$

and its eigenstates (the dressed states) can be expanded with the bare states

$$|D^{(i)}_{n_1,n_2}\rangle = \alpha^{(i)}_{n_1,n_2}|a,n_1,n_2\rangle + \beta^{(i)}_{n_1,n_2}|b,n_1+1,n_2\rangle + \gamma^{(i)}_{n_1,n_2}|c,n_1+1,n_2+1\rangle. \tag{12}$$

Substituting (1) and (12) into (11) we find

$$V^{(0)}_{n_1,n_2} = 0, \qquad V^{(\pm)}_{n_1,n_2} = \pm\Omega_{n_1,n_2}, \tag{13}$$

and

$$\alpha^{(0)}_{n_1,n_2} = \frac{d_2(n_2)}{\Omega_{n_1,n_2}} \quad \beta^{(0)}_{n_1,n_2} = 0 \quad \gamma^{(0)}_{n_1,n_2} = \frac{d_1(n_1)}{\Omega_{n_1,n_2}}$$
$$\alpha^{(+)}_{n_1,n_2} = \frac{d_1(n_1)}{\sqrt{2}\Omega_{n_1,n_2}} \quad \beta^{(+)}_{n_1,n_2} = \frac{1}{\sqrt{2}} \quad \gamma^{(+)}_{n_1,n_2} = \frac{d_2(n_2)}{\sqrt{2}\Omega_{n_1,n_2}}$$
$$\alpha^{(-)}_{n_1,n_2} = \frac{d_1(n_1)}{\sqrt{2}\Omega_{n_1,n_2}} \quad \beta^{(-)}_{n_1,n_2} = -\frac{1}{\sqrt{2}} \quad \gamma^{(-)}_{n_1,n_2} = \frac{d_2(n_2)}{\sqrt{2}\Omega_{n_1,n_2}} \tag{14}$$

where $d_i(n_i)$ and Ω_{n_1,n_2} are defined after equations (5) and (9), respectively.

Suppose that, initially, the atom is in the topmost state $|a\rangle$ and moves along the z-direction with a c.m. momentum k, and the cavity field is in the two-mode Fock state $|n_1,n_2\rangle$, then the initial state for the whole system reads

$$|\Psi_{n_1,n_2}(z,0)\rangle = \theta(-z)\,\mathrm{e}^{\mathrm{i}kz}|a,n_1,n_2\rangle, \tag{15}$$

where the Heaviside unit step function θ merely indicates on which side of the cavity the atom can be found.

For the following discussion, it is expedient to expand this state in terms of the dressed states. By using the inverse of equation (12), we can rewritten (15) as

$$|\Psi_{n_1,n_2}(z,0)\rangle = \theta(-z)\,\mathrm{e}^{\mathrm{i}kz}[\alpha^{(0)}_{n_1,n_2}|D^{(0)}_{n_1,n_2}\rangle + \alpha^{(+)}_{n_1,n_2}|D^{(+)}_{n_1,n_2}\rangle + \alpha^{(-)}_{n_1,n_2}|D^{(-)}_{n_1,n_2}\rangle]. \tag{16}$$

As discussed in [7, 10], the interaction between the slow atom and the cavity field can be treated as a scattering process; the component associated with $|D^{(i)}_{n_1,n_2}\rangle (i=0,\pm)$ encounters a potential $u(z)V^{(i)}_{n_1,n_2}$. In the present case, therefore, the component associated with $|D^{(0)}_{n_1,n_2}\rangle$ will be transmitted through the cavity field freely since $V^{(0)}_{n_1,n_2} = 0$, but the components associated with $|D^{(\pm)}_{n_1,n_2}\rangle$ may be reflected or transmitted since $V^{(\pm)}_{n_1,n_2} = \pm\Omega_{n_1,n_2} \neq 0$. Assume that the reflection amplitudes and the transmission amplitudes for the components associated with $|D^{(\pm)}_{n_1,n_2}\rangle$ are $\rho^{(\pm)}_{n_1,n_2}$ and $\tau^{(\pm)}_{n_1,n_2}$, respectively, then the state of the system after the interaction can be written as

$$|\Psi_{n_1,n_2}(z,\tau)\rangle = \mathrm{e}^{-\mathrm{i}\frac{k^2}{2M}\tau}\{\theta(z-l)\,\mathrm{e}^{\mathrm{i}kz}\alpha^{(0)}_{n_1,n_2}|D^{(0)}_{n_1,n_2}\rangle + [\rho^{(+)}_{n_1,n_2}\theta(-z)\,\mathrm{e}^{-\mathrm{i}kz} + \tau^{(+)}_{n_1,n_2}\theta(z-l)\,\mathrm{e}^{\mathrm{i}kz}]\alpha^{(+)}_{n_1,n_2}|D^{(+)}_{n_1,n_2}\rangle + [\rho^{(-)}_{n_1,n_2}\theta(-z)\,\mathrm{e}^{-\mathrm{i}kz} + \tau^{(-)}_{n_1,n_2}\theta(z-l)\,\mathrm{e}^{\mathrm{i}kz}]\alpha^{(-)}_{n_1,n_2}|D^{(-)}_{n_1,n_2}\rangle\}, \tag{17}$$

where τ is the interaction time between the atom and the cavity field, and l is the cavity length. It should be noted that the definitions of the transmission amplitudes $\tau^{(\pm)}_{n_1,n_2}$ are similar to that in [13], but differ from that in [7] by a factor $\mathrm{e}^{-\mathrm{i}kl}$; the reason for this will be discussed after equation (31).

If the atom–field coupling inside the cavity is constant along the z-direction, then the mode function $u(z)$ can be described by a mesa function

$$u(z) = \begin{cases} 1, & 0 < z < l \\ 0, & \text{elsewhere.} \end{cases} \tag{18}$$

In this case, the reflection amplitudes $\rho^{(\pm)}_{n_1,n_2}$ and the transmission amplitudes $\tau^{(\pm)}_{n_1,n_2}$ can be calculated analytically, and have the following forms:

$$\rho^{(\pm)}_{n_1,n_2} = \mathrm{i}\Delta^{(\pm)}_{n_1,n_2}\sin(k^{(\pm)}_{n_1,n_2}l)[\cos(k^{(\pm)}_{n_1,n_2}l) - \mathrm{i}\Sigma^{(\pm)}_{n_1,n_2}\sin(k^{(\pm)}_{n_1,n_2}l)]^{-1}, \tag{19}$$

$$\tau^{(\pm)}_{n_1,n_2} = \mathrm{e}^{-\mathrm{i}kl}[\cos(k^{(\pm)}_{n_1,n_2}l) - \mathrm{i}\Sigma^{(\pm)}_{n_1,n_2}\sin(k^{(\pm)}_{n_1,n_2}l)]^{-1}, \tag{20}$$

where

$$\Delta^{(\pm)}_{n_1,n_2} = \frac{1}{2}\left(\frac{k^{(\pm)}_{n_1,n_2}}{k} - \frac{k}{k^{(\pm)}_{n_1,n_2}}\right), \qquad \Sigma^{(\pm)}_{n_1,n_2} = \frac{1}{2}\left(\frac{k^{(\pm)}_{n_1,n_2}}{k} + \frac{k}{k^{(\pm)}_{n_1,n_2}}\right), \tag{21}$$

$$k^{(\pm)}_{n_1,n_2} = \sqrt{k^2 \mp k^2_{n_1,n_2}}, \qquad k_{n_1,n_2} = \sqrt{2M\Omega_{n_1,n_2}}. \tag{22}$$

We note that the expressions of the transmission amplitudes $\tau^{(\pm)}_{n_1,n_2}$ are similar to that in [13], but differ from that in [7] by a factor $\mathrm{e}^{-\mathrm{i}kl}$; the reason for this will be discussed after equation (31).

For the following discussion, we now transform (17) back into the bare-state basis by using (12)

$$|\Psi_{n_1,n_2}(z,\tau)\rangle = \mathrm{e}^{-\mathrm{i}\frac{k^2}{2M}\tau}\{[R_{a,n_1,n_2}\theta(-z)\,\mathrm{e}^{-\mathrm{i}kz} + T_{a,n_1,n_2}\theta(z-l)\,\mathrm{e}^{\mathrm{i}kz}]|a,n_1,n_2\rangle + [R_{b,n_1+1,n_2}\theta(-z)\,\mathrm{e}^{-\mathrm{i}kz} + T_{b,n_1+1,n_2}\theta(z-l)\,\mathrm{e}^{\mathrm{i}kz}] \times|b,n_1+1,n_2\rangle + [R_{c,n_1+1,n_2+1}\theta(-z)\,\mathrm{e}^{-\mathrm{i}kz} + T_{c,n_1+1,n_2+1}\theta(z-l)\,\mathrm{e}^{\mathrm{i}kz}]|c,n_1+1,n_2+1\rangle\}, \tag{23}$$

where

$$R_{a,n_1,n_2} = \frac{1}{2}\left(\frac{d_1(n_1)}{\Omega_{n_1,n_2}}\right)^2\left(\rho^{(+)}_{n_1,n_2} + \rho^{(-)}_{n_1,n_2}\right), \tag{24}$$

$$T_{a,n_1,n_2} = \frac{1}{2}\left(\frac{d_1(n_1)}{\Omega_{n_1,n_2}}\right)^2\left[\left(\tau^{(+)}_{n_1,n_2} + \tau^{(-)}_{n_1,n_2}\right) + 2\left(\frac{d_2(n_2)}{d_1(n_1)}\right)^2\right], \tag{25}$$

$$R_{b,n_1+1,n_2} = \frac{1}{2}\frac{d_1(n_1)}{\Omega_{n_1,n_2}}\left(\rho^{(+)}_{n_1,n_2} - \rho^{(-)}_{n_1,n_2}\right), \tag{26}$$

$$T_{b,n_1+1,n_2} = \frac{1}{2}\frac{d_1(n_1)}{\Omega_{n_1,n_2}}\left(\tau^{(+)}_{n_1,n_2} - \tau^{(-)}_{n_1,n_2}\right), \tag{27}$$

$$R_{c,n_1+1,n_2+1} = \frac{1}{2}\frac{d_1(n_1)d_2(n_2)}{\Omega^2_{n_1,n_2}}\left(\rho^{(+)}_{n_1,n_2} + \rho^{(-)}_{n_1,n_2}\right), \tag{28}$$

$$T_{c,n_1+1,n_2+1} = \frac{1}{2}\frac{d_1(n_1)d_2(n_2)}{\Omega^2_{n_1,n_2}}\left[\left(\tau^{(+)}_{n_1,n_2} + \tau^{(-)}_{n_1,n_2}\right) - 2\right], \tag{29}$$

in which equation (14) has been used. Here R_{a,n_1,n_2} (R_{b,n_1+1,n_2}, R_{c,n_1+1,n_2+1}) and T_{a,n_1,n_2} (T_{b,n_1+1,n_2}, T_{c,n_1+1,n_2+1}) are the reflection amplitude and the transmission amplitude of the

bare state $|a, n_1, n_2\rangle$ ($|b, n_1 + 1, n_2\rangle$, $|c, n_1 + 1, n_2 + 1\rangle$) after the interaction, respectively.

In the fast-atom limit, $k^2 \gg k_{n_1,n_2}^2$, in turn, $k_{n_1,n_2}^{(\pm)} \approx k \mp k_{n_1,n_2}^2/2k$, $\Delta_{n_1,n_2}^{(\pm)} \approx 0$, $\Sigma_{n_1,n_2}^{(\pm)} \approx 1$, $\rho_{n_1,n_2}^{(\pm)} \approx 0$ and $\tau_{n_1,n_2}^{(\pm)} \approx \mathrm{e}^{\mathrm{i}k_{n_1,n_2}^{(\pm)}}\mathrm{e}^{-\mathrm{i}kl} \approx \exp(\mp\mathrm{i}k_{n_1,n_2}^2 l/2k) = \exp(\mp\mathrm{i}\Omega_{n_1,n_2}\tau)$; therefore, we obtain

$$R_{a,n_1,n_2} = R_{b,n_1+1,n_2} = R_{c,n_1+1,n_2+1} = 0, \tag{30}$$

$$T_{a,n_1,n_2} = C_{a,n_1,n_2}(\tau), \qquad T_{b,n_1+1,n_2} = C_{b,n_1+1,n_2}(\tau), \qquad T_{c,n_1+1,n_2+1} = C_{c,n_1+1,n_2+1}(\tau), \tag{31}$$

where C_{a,n_1,n_2}, C_{b,n_1+1,n_2} and C_{c,n_1+1,n_2+1} are given by equations (7)–(9), respectively. These results are obviously reasonable. In the fast-atom limit, corresponding to the atomic kinetic energy, the potential barrier encountered by the positive component is very low and the potential well met by the negative component is very shallow; therefore, the atom will not be reflected, it will only be transmitted. In other words, it is not necessary to treat the c.m. motion of the atom quantum mechanically in the fast-atom limit. This issue has been proved by the agreement between the theories and the experiments of the micromaser injected with thermal atoms [14]. If we had not used the definitions of the transmission amplitudes $\tau_{n_1,n_2}^{(\pm)}$ as that in [13], we would not have obtained equation (31), and this would affect the calculations of other physical quantities. However, it can be shown that the two definitions of the transmission amplitudes are equivalent for the two-level one-photon maser [7], and for the three-level two-photon maser [8] in the slow-atom limit.

4. Atom dynamics: analytical discussion

Now we study the dynamics of the system. After the atom–field interaction, the probability of the system being in the state $|b, n_1 + 1, n_2\rangle$ is

$$P_{b,n_1+1,n_2} = |R_{b,n_1+1,n_2}|^2 + |T_{b,n_1+1,n_2}|^2. \tag{32}$$

By using equations (26), (27) and (19), (20) we obtain

$$P_{b,n_1+1,n_2} = \frac{1}{2}\left(\frac{d_1(n_1)}{\Omega_{n_1,n_2}}\right)^2 \left\{1 - \frac{F_{n_1,n_2}^{(1)} F_{n_1,n_2}^{(2)}}{E_{n_1,n_2}^{(+)} E_{n_1,n_2}^{(-)}}\right\} \tag{33}$$

where

$$\begin{aligned} F_{n_1,n_2}^{(1)} &= 1 + \Delta_{n_1,n_2}^{(+)}\Delta_{n_1,n_2}^{(-)} S_{n_1,n_2}^{(+)} S_{n_1,n_2}^{(-)}, \\ F_{n_1,n_2}^{(2)} &= C_{n_1,n_2}^{(+)} C_{n_1,n_2}^{(-)} + \Sigma_{n_1,n_2}^{(+)}\Sigma_{n_1,n_2}^{(-)} S_{n_1,n_2}^{(+)} S_{n_1,n_2}^{(-)}, \\ E_{n_1,n_2}^{(\pm)} &= (C_{n_1,n_2}^{(\pm)})^2 + (\Sigma_{n_1,n_2}^{(\pm)} S_{n_1,n_2}^{(\pm)})^2, \\ C_{n_1,n_2}^{(\pm)} &= \cos(k_{n_1,n_2}^{(\pm)} l), \qquad S_{n_1,n_2}^{(\pm)} = \sin(k_{n_1,n_2}^{(\pm)} l). \end{aligned} \tag{34}$$

Equation (33) with (34) looks like the expression for the emission probability in the one-photon maser [7], but the differences are also evident. We can also calculate the probability of the system being in the state $|c, n_1 + 1, n_2 + 1\rangle$ after the interaction,

$$P_{c,n_1+1,n_2+1} = |R_{c,n_1+1,n_2+1}|^2 + |T_{c,n_1+1,n_2+1}|^2. \tag{35}$$

By using equations (28), (29) and (19), (20) we obtain

$$P_{c,n_1+1,n_2+1} = \frac{1}{2}\left(\frac{d_1(n_1)d_2(n_2)}{\Omega_{n_1,n_2}^2}\right)^2 \left\{3 + \frac{F_{n_1,n_2}^{(1)} F_{n_1,n_2}^{(2)}}{E_{n_1,n_2}^{(+)} E_{n_1,n_2}^{(-)}} - \frac{2}{E_{n_1,n_2}^{(+)} E_{n_1,n_2}^{(-)}}\left[F_{n_1,n_2}^{(3)} + F_{n_1,n_2}^{(4)}\right]\right\}, \tag{36}$$

where

$$\begin{aligned} F_{n_1,n_2}^{(3)} &= (C_{n_1,n_2}^{(+)} E_{n_1,n_2}^{(-)} + C_{n_1,n_2}^{(-)} E_{n_1,n_2}^{(+)}) \cos kl, \\ F_{n_1,n_2}^{(4)} &= (\Sigma_{n_1,n_2}^{(+)} S_{n_1,n_2}^{(+)} E_{n_1,n_2}^{(-)} + \Sigma_{n_1,n_2}^{(-)} S_{n_1,n_2}^{(-)} E_{n_1,n_2}^{(+)}) \sin kl. \end{aligned} \tag{37}$$

The information about the probability of the system being in the state $|a, n_1, n_2\rangle$ can be obtained from the relation $P_{a,n_1,n_2} + P_{b,n_1+1,n_2} + P_{c,n_1+1,n_2+1} = 1$. Equations (33) and (36) are rather complicated; we shall use them only in the numerical calculations. For analytical discussion we consider some limit cases.

4.1. Fast-atom limit

In the fast-atom limit, by substituting equations (30), (31) and (7)–(9) into (32) and (35), we obtain

$$P_{b,n_1+1,n_2} = \left(\frac{d_1(n_1)}{\Omega_{n_1,n_2}}\right)^2 \sin^2(\Omega_{n_1,n_2}\tau), \tag{38}$$

$$P_{c,n_1+1,n_2+1} = \left(\frac{d_1(n_1)d_2(n_2)}{\Omega_{n_1,n_2}^2}\right)^2 [1 - \cos(\Omega_{n_1,n_2}\tau)]^2. \tag{39}$$

These results are in agreement with previous works [11].

4.2. Slow-atom limit

In the slow-atom limit, $k^2 \ll k_{n_1,n_2}^2$, in turn, $k_{n_1,n_2}^{(-)} \approx k_{n_1,n_2}$, $k_{n_1,n_2}^{(+)} \approx \mathrm{i}k_{n_1,n_2}$, $\Delta_{n_1,n_2}^{(-)} \approx \Sigma_{n_1,n_2}^{(-)} \approx k_{n_1,n_2}/2k \equiv f_{n_1,n_2} \gg 1$, $\Delta_{n_1,n_2}^{(+)} \approx \Sigma_{n_1,n_2}^{(+)} \approx \mathrm{i}f_{n_1,n_2}$. In this case we have

$$\rho_{n_1,n_2}^{(+)} \approx -1, \qquad \tau_{n_1,n_2}^{(+)} \approx 0, \tag{40}$$

$$\rho_{n_1,n_2}^{(-)} = \mathrm{i}f_{n_1,n_2}\sin(k_{n_1,n_2}l)[\cos(k_{n_1,n_2}l) - \mathrm{i}f_{n_1,n_2}\sin(k_{n_1,n_2}l)]^{-1}, \tag{41}$$

$$\tau_{n_1,n_2}^{(-)} = \mathrm{e}^{-\mathrm{i}kl}[\cos(k_{n_1,n_2}l) - \mathrm{i}f_{n_1,n_2}\sin(k_{n_1,n_2}l)]^{-1}. \tag{42}$$

Equation (40) shows that, in the slow-atom limit, corresponding to the atomic kinetic energy, the potential barrier encountered by the positive component is very high; therefore, the positive component will be reflected almost fully. Substituting equations (40)–(42) into (26), (27), and in turn into (32), we obtain

$$P_{b,n_1+1,n_2} = \frac{1}{2}\left(\frac{d_1(n_1)}{\Omega_{n_1,n_2}}\right)^2 \frac{1}{1 + f_{n_1,n_2}^2 \sin^2(k_{n_1,n_2}l)}. \tag{43}$$

By comparing equation (38) with equation (43) we find that the probability depends on the interaction time τ in the fast-atom limit, while it depends on the interaction length l (the cavity length) in the slow-atom limit. Equation (43) resembles the Airy function of classical optics, $[1 + F\sin^2(\Delta_\mathrm{p}/2)]^{-1}$, which gives the transmitted intensity in a Fabry–Perot interferometer with finesse F and total phase difference Δ_p [12]. In our

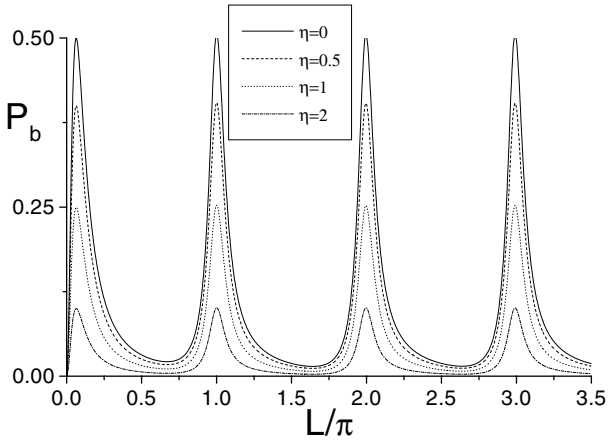

Figure 2. The population probability P_b versus the dimensionless cavity length L with the parameters: $K = 0.1$, $n_1 = n_2 = 0$ and $\eta = 0$, 0.5, 1 and 2, respectively.

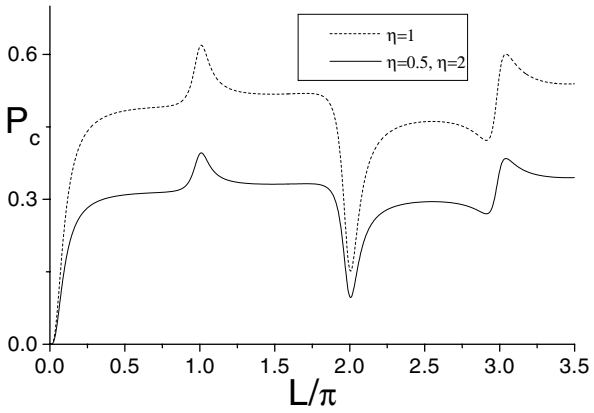

Figure 3. The population probability P_c versus the dimensionless cavity length L with the parameters: $K = 0.1$, $n_1 = n_2 = 0$ and $\eta = 0.5$ and 1, respectively. $P_c = 0$ for $\eta = 0$, and the curve for $\eta = 2$ overlaps with that for $\eta = 0.5$.

situation here, $F = f_{n_1,n_2}^2 = (k_{n_1,n_2}/2k)^2$ and $\Delta_{\rm p} = 2k_{n_1,n_2}l$. There will appear resonant peaks when $k_{n_1,n_2}l = m\pi$ (m is an integer). We note that, besides the common factor k_{n_1,n_2}, $\Delta_{\rm p}$ is proportional to the cavity length l, while F is inversely proportional to the square of the c.m. momentum, i.e. $F \propto 1/k^2$, so the resonant peaks of P_{b,n_1+1,n_2} will become sharper when the atom moves more slowly (k is smaller).

In fact, under the slow-atom limit, $f_{n_1,n_2} = k_{n_1,n_2}/2k \gg 1$, we find from (41) and (42) that $\rho_{n_1,n_2}^{(-)} = 0$ and $|\tau_{n_1,n_2}^{(-)}| = 1$ when the resonant condition $k_{n_1,n_2}l = m\pi$ is met, while $|\rho_{n_1,n_2}^{(-)}| \approx 1$ and $\tau_{n_1,n_2}^{(-)} \approx 0$ when the resonant condition is not met. The resonant condition $k_{n_1,n_2}l = m\pi$ corresponds to $l = m\,\lambda_{n_1,n_2}/2$, where $\lambda_{n_1,n_2} = 2\pi/k_{n_1,n_2}$ is the de Broglie wavelength of the atom in the cavity. Therefore, the negative component will transmit through the cavity fully when the cavity length is an integer multiple of half the de Broglie wavelength; otherwise, it will be reflected almost fully.

5. Atom dynamics: influences of initial fields

In the above discussions we assumed that the field is initially in the two-mode Fock state $|n_1, n_2\rangle$. When the field is initially in a state with a photon number distribution $P_{n_1,n_2}(0)$, then the probabilities of the atom in the state $|b\rangle$ and $|c\rangle$ will be

$$P_b = \sum_{n_1,n_2} P_{n_1,n_2}(0)\,P_{b,n_1+1,n_2}, \tag{44}$$

and

$$P_c = \sum_{n_1,n_2} P_{n_1,n_2}(0)\,P_{c,n_1+1,n_2+1}, \tag{45}$$

respectively.

In the following we consider several initial field states and give a discussion from numerical calculations. Since the properties for the thermal-atom (fast-atom) case are well known from previous works [11], here we concentrate our attention mainly on the ultracold-atom (slow-atom) situation.

For convenience, in the numerical calculations we have introduced $\varkappa = \sqrt{2M\sqrt{g_1^2 + g_2^2}}$, which has the dimension of a momentum, and $\varkappa^2/2M = \sqrt{g_1^2 + g_2^2}$ is the vacuum coupling energy (note that we have taken $\hbar = 1$). We have also introduced the dimensionless c.m. momentum $K = k/\varkappa$, the dimensionless cavity length $L = \varkappa l$ and the ratio of the two coupling constants $\eta = g_2/g_1$. Using these quantities in equation (43) we can obtain the width of the resonance peaks $(2\Delta L)_{\rm FWHM} = 4K\{[(n_1+1) + \eta^2(n_2+1)]/(1+\eta^2)\}^{-1/2}$. We see that the peaks become sharper when the atom changes slower (K changes smaller) and/or the field changes stronger (n_1 and/or n_2 change/changes larger).

Case a. Initially, both modes are in the vacuum state, i.e. $n_1 = 0$, and $n_2 = 0$. This situation corresponds to the cascade two-mode spontaneous emission. The variations of the probabilities versus L, with n_1, n_2, K and η as parameters, are shown in figures 2 and 3. In the numerical calculations the exact expressions (33) and (36) have been used, but the value of K is for the slow-atom region ($K < 1$, i.e. $k < \varkappa$). We see from figure 2 that the probability P_{b,n_1+1,n_2} shows resonant peaks at $L = m\pi (m = 1, 2, \ldots)$. This is in agreement with equation (43) and the discussions following it. Here it should be pointed out that the approximate expression (43) is not suitable near $L = 0$. We also see that P_{b,n_1+1,n_2} decreases monotonically as η increases. This is because the increase of η will speed up the depletion of the population in the atomic state $|b\rangle$. However, we see from figure 3 that P_{c,n_1+1,n_2+1} does not change monotonically with η. In fact, the curves for $\eta = 2$ and for $\eta = 0.5$ are fully overlapping. This is because we have taken $n_1 = n_2$, and under this condition the two situations $\eta = 2$ ($g_2 = 2g_1$) and $\eta = 0.5$ ($g_1 = 2g_2$) are equivalent for the population in the atomic state $|c\rangle$.

In order to lay stress on the influences of the initial field states and initial field intensity, we take $\eta = 1$ (i.e. $g_1 = g_2$) in the following cases b, c and d.

Case b. Initially, mode 1 is in the vacuum state, i.e. $n_1 = 0$, while mode 2 is in a coherent state; the initial photon number distribution $P_{n_1,n_2}(0)$ can be written as

$$P_{n_1,n_2}(0) = \delta_{n_1,0}\exp(-\langle n_2\rangle)\frac{\langle n_2\rangle^{n_2}}{n_2!}, \tag{46}$$

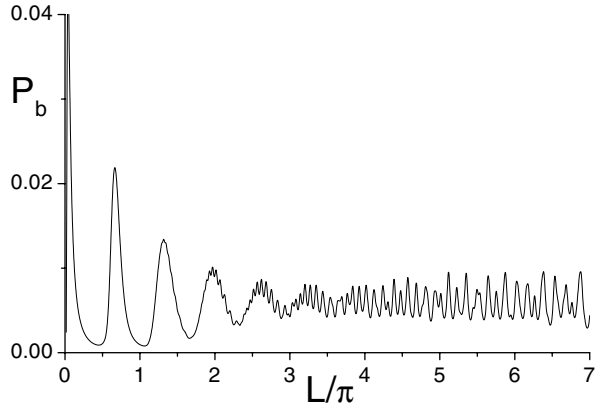

Figure 4. P_b versus L with the parameters $K = 0.1$, $\eta = 1$, $n_1 = 0$ and $\langle n_2 \rangle = 10$.

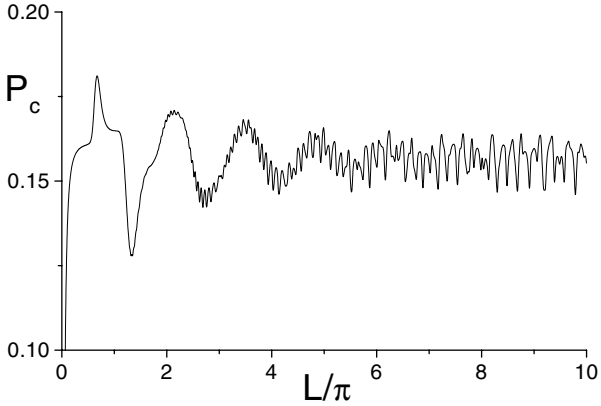

Figure 5. P_c versus L with the parameters $K = 0.1$, $\eta = 1$, $n_1 = 0$ and $\langle n_2 \rangle = 10$.

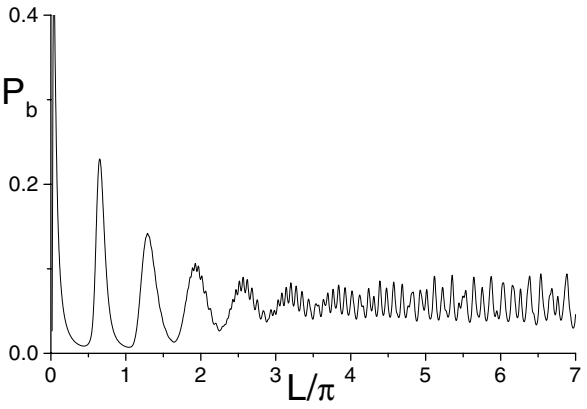

Figure 6. P_b versus L with the parameters $K = 0.1$, $\eta = 1$, $\langle n_1 \rangle = 10$ and $n_2 = 0$.

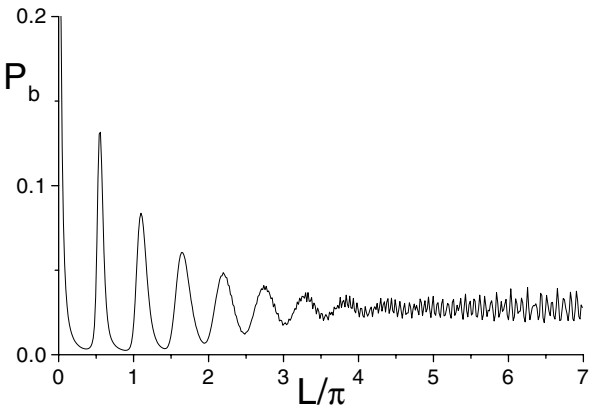

Figure 7. P_b versus L with the parameters $K = 0.1$, $\eta = 1$ and $\langle n_1 \rangle = \langle n_2 \rangle = 10$.

where $\langle n_2 \rangle$ is the initial mean photon number in mode 2. The variations of the probabilities versus L are shown in figures 4 and 5. Comparing with the curve for $\eta = 1$ in figure 2 we find that the amplitude of P_b in figure 4 decreases. There are two reasons for this. Firstly, in this case, mode 2 is stronger than mode 1 ($\langle n_2 \rangle = 10, n_1 = 0$); this speeds up the depletion of the population in the state $|b\rangle$. Secondly, we know from the resonant condition $k_{n_1,n_2} l = m\pi$ that the resonant peaks for different (n_1, n_2) appear at different places; the summation over n_2 makes P_b collapse. However, for P_c, the effects of the two factors are opposite. The increase of the intensity of mode 2 makes P_c increase, while the summation over n_2 makes it collapse. The variation is shown in figure 5. The second reason also makes the variations of the probabilities versus L change faster.

Case c. Initially, mode 2 is in the vacuum state, i.e. $n_2 = 0$, while mode 1 is in a coherent state; the initial photon number distribution $P_{n_1,n_2}(0)$ can be written as

$$P_{n_1,n_2}(0) = \delta_{n_2,0} \exp(-\langle n_1 \rangle) \frac{\langle n_1 \rangle^{n_1}}{n_1!}, \tag{47}$$

where $\langle n_1 \rangle$ is the initial mean photon number in mode 1. The variation of P_b versus L is shown in figure 6. Comparing with figure 4 we find that the amplitude of P_b in figure 6 increases. This is because, in this case, mode 1 is stronger than mode 2 ($\langle n_1 \rangle = 10, n_2 = 0$); this strengthens the transition $|a\rangle \to |b\rangle$, and weakens the transition $|b\rangle \to |c\rangle$. For P_c, under the condition $\eta = 1$ ($g_1 = g_2$), the curve for the parameters $\langle n_1 \rangle = 10, n_2 = 0$ is identical with that for the parameters $\langle n_2 \rangle = 10, n_1 = 0$ in case b above (i.e. figure 5). This means that the two situations are equivalent for P_c under the condition $\eta = 1$. The effects of the summation are the same as in case b.

Case d. Initially, both modes are in coherent states; the initial photon number distribution $P_{n_1,n_2}(0)$ can be written as

$$P_{n_1,n_2}(0) = \exp(-\langle n_1 \rangle) \frac{\langle n_1 \rangle^{n_1}}{n_1!} \exp(-\langle n_2 \rangle) \frac{\langle n_2 \rangle^{n_2}}{n_2!}. \tag{48}$$

The variations of P_b and P_c versus L are shown in figures 7 and 8, respectively. In these two figures, the parameters for the two modes are identical ($\eta = 1, \langle n_1 \rangle = \langle n_2 \rangle = 10$). Comparing figure 7 with figures 4 and 6 we find that the values of P_b in figure 7 are larger than that in figure 4, but smaller than that in figure 6. This is due to the competition between the two transitions. However, for P_c, the two transitions are cooperative; this can be seen by comparing figure 8 with figure 5: the values of P_c in figure 8 are larger than that in figure 5. The double summations make the variations of the probabilities versus L change more quickly.

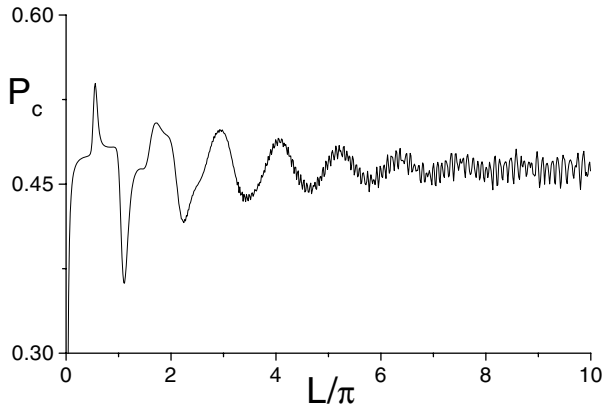

Figure 8. P_c versus L with the parameters $K = 0.1$, $\eta = 1$ and $\langle n_1 \rangle = \langle n_2 \rangle = 10$.

6. Summary

We have studied the interaction between an ultracold cascade three-level atom and a two-mode cavity field, and examined the effects of some parameters on the atomic dynamics. The main results are summarized as follows: the population probabilities show dependence on the interaction time τ in the fast-atom region while they show dependence on the interaction length (the cavity length) L in the slow-atom region. The variations of the probabilities versus L show some resonant peaks. The resonant peaks become sharper as the atom moves more slowly (the c.m. momentum K is smaller). When the ratio of the two coupling constants ($\eta = g_2/g_1$) increases, the probability P_b decreases monotonically, while P_c does not behave this way. The initial field states and the initial field intensity also influence the atomic dynamics significantly. The two transitions are competitive for P_b, while cooperative for P_c. The results of this paper may be tested with micromaser-like experiments [7, 14].

Acknowledgments

This work was supported by the National Natural Science Foundation of China under grant no 10074046 and 60178001, and by the National Science Council of China under grant no NSC 89-2816-E-009-0005-6.

References

[1] For reviews see Chu S 1998 *Rev. Mod. Phys.* **70** 685
Cohen-Tannoudji C N 1998 *Rev. Mod. Phys.* **70** 707
Phillips W D 1998 *Rev. Mod. Phys.* **70** 721
Wieman C E, Pritchard D E and Wineland J 1999 *Rev. Mod. Phys.* **71** S253
Arimondo E, Phillips W D and Strumia F (ed) 1992 *Laser Manipulation of Atoms and Ions* (Amsterdam: North-Holland)
[2] For reviews see: Adams C, Sigel M and Mlynek J 1994 *Phys. Rep.* **240** 143
Balykin V I and Letokhov V S 1995 *Atom Optics with Laser Light* (Switzerland: Harwood)
[3] Anderson M H *et al* 1995 *Science* **269** 198
Bradley C C *et al* 1995 *Phys. Rev. Lett.* **75** 1687
Davis B K *et al* 1995 *Phys. Rev. Lett.* **75** 3969
Griffin A, Snoke D W and Stringari S (ed) 1995 *Bose–Einstein Condensation* (Cambridge: Cambridge University Press)
[4] Andrews M R *et al* 1997 *Science* **275** 637
Hagley E W *et al* 1999 *Science* **283** 1702
Bloch I, Hansch T W and Esslinger T 1999 *Phys. Rev. Lett.* **82** 3008
[5] Lenz G, Meystre P and Wright E M 1994 *Phys. Rev.* A **50** 1681
[6] Goldstein E V, Moore M G and Meystre P 2000 Nonlinear optics of matter waves *Advances in Laser Physics* ed V S Letokhov and P Meystre (Amsterdam: Harwood) p 117
[7] Scully M O, Meyer G M and Walther H 1996 *Phys. Rev. Lett.* **76** 4144
Meyer G M, Scully M O and Walther H 1997 *Phys. Rev.* A **56** 4142
Loffler M *et al* 1997 *Phys. Rev.* A **56** 4153
Schroder M *et al* 1997 *Phys. Rev.* A **56** 4164
Loffler M, Meyer G M and Walther H 1998 *Europhys. Lett.* **41** 593
[8] Zhang Z M and He L S 1998 *Opt. Commun.* **157** 77
Zhang Z M, Lu Z Y and He L S 1999 *Phys. Rev.* A **59** 808
Zhang Z M, Xie S W and Zhou S K 1999 *J. Phys. B: At. Mol. Opt. Phys.* **32** 4013
Zhang Z M *et al* 1999 *Phys. Rev.* A **60** 3321
Zhang Z M *et al* 1999 *J. Phys. B: At. Mol. Opt. Phys.* **33** 2125
[9] Aran R, Agarwal G S, Scully M O and Walther H 2000 *Phys. Rev.* A **62** 023809
[10] Horache S, Brune M and Raimond J M 1991 *Europhys. Lett.* **14** 19
Englert B-G, Schwinger J, Barut A O and Scully M O 1991 *Europhys. Lett.* **14** 25
[11] See for example Shore B W and Knight P L 1993 *J. Mod. Opt.* **40** 1195
Yoo H-I and Eberly J H 1985 *Phys. Rep.* **118** 239
[12] Born M and Wolf E 1980 *Principles of Optics* 6th edn (New York: Pergamon)
[13] Schwabl F 1992 *Quantum Mechanics* (Berlin: Springer)
[14] For reviews on the micromaser see Walther H 2000 *Frontiers Laser Physics and Quantum Optics* ed Z Z Xu, S W Xie, S Y Zhu and M O Scully (Berlin: Springer) p 39
Raithel G *et al* 1994 *Cavity Quantum Electrodynamics* ed P R Berman (Boston: Academic) p 57
[15] Brune M *et al* 1996 *Phys. Rev. Lett.* **76** 1800